



LUND UNIVERSITY

Ion pairing and phase behaviour of an asymmetric restricted primitive model of ionic liquids

Lu, Hongduo; Li, Bin; Nordholm, Sture; Woodward, Clifford E.; Forsman, Jan

Published in:
Journal of Chemical Physics

DOI:
[10.1063/1.4972214](https://doi.org/10.1063/1.4972214)

2016

[Link to publication](#)

Citation for published version (APA):

Lu, H., Li, B., Nordholm, S., Woodward, C. E., & Forsman, J. (2016). Ion pairing and phase behaviour of an asymmetric restricted primitive model of ionic liquids. *Journal of Chemical Physics*, 145(23), Article 234510. <https://doi.org/10.1063/1.4972214>

Total number of authors:
5

General rights

Unless other specific re-use rights are stated the following general rights apply:

Copyright and moral rights for the publications made accessible in the public portal are retained by the authors and/or other copyright owners and it is a condition of accessing publications that users recognise and abide by the legal requirements associated with these rights.

- Users may download and print one copy of any publication from the public portal for the purpose of private study or research.
- You may not further distribute the material or use it for any profit-making activity or commercial gain
- You may freely distribute the URL identifying the publication in the public portal

Read more about Creative commons licenses: <https://creativecommons.org/licenses/>

Take down policy

If you believe that this document breaches copyright please contact us providing details, and we will remove access to the work immediately and investigate your claim.

LUND UNIVERSITY

PO Box 117
221 00 Lund
+46 46-222 00 00

Ion Pairing and Phase Behaviour of an Asymmetric Restricted Primitive Model of Ionic Liquids

Hongduo Lu^{†1}, Bin Li^{†1}, Sture Nordholm², Clifford E. Woodward³, and Jan
Forsman^{1*}

¹*Theoretical Chemistry, Lund University, P.O.Box 124, S-221 00 Lund, Sweden*

²*Department of Chemistry, The University of Gothenburg, SE-412 96 Göteborg, Sweden*

³*School of Physical, Environmental and Mathematical Sciences, University of New South Wales,
Canberra, ACT 2600, Australia*

[†] *Contributed equally to the work.*

E-mail: jan.forsman@teokem.lu.se

Abstract

An asymmetric restricted primitive model (ARPM) of electrolytes is proposed as a simple three parameter (charge q , diameter d and charge displacement b) model of ionic liquids and solutions. Charge displacement allows electrostatic and steric interactions to operate between different centres, so that orientational correlations arise in ion-ion interactions. In this way the ionic system may have partly the character of a simple ionic fluid/solid and of a polar fluid formed from ion pairs. The present exploration of the system focuses on the ion pair formation mechanism, the relative concentration of paired and free ions and the consequences for the cohesive energy, and the tendency to form fluid or solid phase. In contrast to studies of similar (though not identical) models in the past, we focus on behaviours at room temperature. By MC and MD simulations of such systems composed of monovalent ions of hard-sphere (or

*To whom correspondence should be addressed

essentially hard-sphere) diameter equal to 5 Å and a charge displacement from hard-sphere origin ranging from 0 to 2 Å we find that ion pairing dominates for b larger than 1 Å. When b exceeds about 1.5 Å, the system is essentially a liquid of dipolar ion pairs, with a small presence of free ions. We also investigate dielectric behaviours of corresponding liquids, composed of purely dipolar species. Many basic features of ionic liquids appear to be remarkably consistent with those of our ARPM at ambient conditions, when b is around 1 Å. However, the rate of self-diffusion and, to a lesser extent, conductivity are overestimated, presumably due to the simple spherical shape of our ions in the ARPM. The relative simplicity of our ARPM in relation to the rich variety of new mechanisms and properties it introduces, and to the numerical simplicity of its exploration by theory or simulation, makes it an essential step on the way towards representation of the full complexity of ionic liquids.

Introduction

The so-called restricted primitive model (RPM) has been widely applied to aqueous salt solutions and dispersions of charged particles. The model is a crude one, e.g., the solvent is treated as a dielectric continuum while all the ions are hard spheres, with diameter d , each carrying a charge $\pm q$, embedded at the center. While its relative simplicity may detract from its ability to describe say specific effects in electrolytes, steric and electrostatic interactions are clearly articulated in the model and the RPM has been instrumental to our understanding of how these mechanisms interact in simple electrolytes. The model has also been utilized to describe molten salts and other types of ionic liquids, wherein steric and electrostatic correlations have uncovered effects that are sensitive to temperature, dielectric response and ion concentration.

The logical next step towards a more realistic modelling of electrolytes and ionic liquids (ILs) is simple generalization of the RPM. Several modified RPM models, have been proposed which allow other mechanisms to be explored. For instance, Spohr and Patey performed studies on charged Lennard-Jones particles with size-asymmetry,¹ charge-asymmetry, competing influences of size and charge asymmetry,² and solvent polarization.³ [Lindenberg and Spohr also simulated melt-](#)

ing temperatures for systems containing charge-asymmetric Lennard-Jones ions.⁴ In a subsequent study, they investigated effects of size-asymmetry.⁵ Malvaldi and Chiappe introduced a dumb-bell model.⁶ Slivestre-Alcantara and co-workers performed analyses on mixtures of off-centre charged cations and centrally charged anions⁷, as well as on ions composed of hard-sphere dimers, where only one of the tangentially connected spheres carry a charge.⁸ Similar models, also including those with a trimer structure, were considered by Fedorov and Kornyshev.^{9,10} Models with Gaussian-distributed charges have also been considered.^{11,12}

In room temperature ionic liquids (RTILs), a high density and low dielectric screening promotes large electrostatic correlations and the increased importance of steric interactions. Here the RPM (and modifications to it) can serve as a basic model that can be treated semi-analytically or numerically with simulations. However, it is clear that the simple RPM does not include the mechanisms responsible for the persistent fluidity of RTILs. Instead, quite detailed molecular models are often proposed, which are typically investigated using simulations, the results of which can be difficult to interpret in terms of basic mechanisms. The purpose of our current work is to find the simplest extension of the RPM, which includes the most essential mechanisms responsible for the properties of RTILs. In particular, we will investigate a model that is very close to the original RPM but which includes a new parameter, b , (common to all ions) which measures the displacement of the charge away from the center of the hard sphere ($b \leq d/2$). Of particular interest to us will be how b influences the freezing point and overall cohesion within an ionic liquid. For example, one can anticipate that a significant displacement of charge away from the center will result in the formation of ion pairs, which in turn can have a considerable influence on electrostatic screening. There are surface force, conductivity and voltammetry measurements that do support the existence of ion pairs, or higher order clusters, in ionic liquids.^{11–16} For example, Gebbie *et al.*^{11,12} used the Surface Force Apparatus, SFA, to measure interactions between charged surfaces, separated by ILs. They found long-ranged forces, persisting to separations of 10–12 nm. If one assumes these forces can be explained by simple electrostatic screening arguments, the implied fraction of free (unassociated) ions would be below 0.1 %. Interestingly, Smith *et al.*¹⁶ performed

SFA studies of simple aqueous salt solutions, and noted an *increased* range of the forces with added salt, for concentrated solutions (beyond some threshold value). Their measurements also confirmed the existence of long-ranged interactions in RTILs, and in concentrated RTIL+solvent mixtures. A correlation between transport properties and ion pair (or cluster) formation in RTILs has been found in simulations.^{17,18} Sha *et al.* simulated RTILs in aqueous solutions as well as the corresponding neat liquid. They found strong ion association in the latter and in highly concentrated solutions. However, the average life-time of the clusters was estimated to be relatively short - of the order of nanoseconds. The fact that RTILs display a significant conductivity seems to be at odds with the conjecture of almost complete association. It is true that the conductivity is generally lower than one would anticipate in a fully dissociated fluid, but a degree of association of about 50 percent normally suffices to explain the measured values. While it is possible that charge transfer^{15,19} can at least offer a partial explanation for these discrepancies, there seems to be little overall consensus about this issue in the presence of seemingly contradictory experimental results.

The formation of ion pairs, i.e. dimers, may be expected to impart the following properties to the fluid:

- a reduced tendency to freeze into a crystal
- a reduced conductivity
- a reduced electrostatic screening, i.e. an increased range of the electrostatic interactions
- a dielectric low frequency response of the fluid

We also anticipate interesting new behaviours in heterogeneous systems, e.g. in the vicinity of charged or neutral electrodes. These aspects will be investigated in a subsequent publication.

While our model contains two parameters (the ionic radius d and the charge displacement distance b), for molar volumes typical of RTILs at atmospheric pressure, d is realistically constrained within a rather narrow window of values. Hence, we are in effect left with one freely varying parameter, b . In this study, we focus on fundamental aspects of the bulk fluid, such as the melting

point, dielectric response, structure, cohesion, diffusion and conductivity. We will consider how these properties vary with b , and compare the results with those typical for RTILs. We will also address the role of ion pairing in some detail. We used Metropolis Monte Carlo (MC) simulations and the veracity of the results were ascertained by comparing with Molecular Dynamics (MD) calculations. MC simulation codes are less amenable to efficient parallelization, so MD simulations tended to be more efficient, at least given our access to a computational cluster.

While this work is primarily devoted to generic ARPM models of RTILs, it should be emphasized that the ARPM also may constitute an interesting extension to the RPM model of aqueous salt solutions. We anticipate relevant contributions to osmotic and activity coefficients, as well as to the screening properties and capacitance of such solutions. However, we postpone these considerations to future work.

The model is described in the next section, followed by the presentation of results. We conclude with a discussion and suggestions for future studies.

Model and methods

The model we use here adheres to the simple RPM description, with a common hard sphere diameter d and charge $\pm q$ for the ions, maintaining electroneutrality.

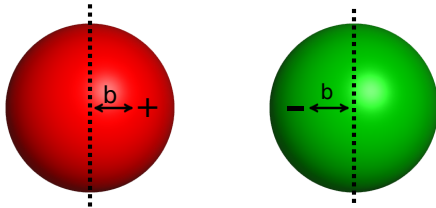


Figure 1: A graphical illustration of the ARPM, being composed of hard-sphere ions, each carrying a charge that is displaced a distance b from the centre.

In this work, we shall only consider monovalent charges, i.e., q is equal to the elementary charge. In future work, fractional charges may also feature, given the possibility that charge transfer may play a role in RTILs.^{15,19} In this context, we note that varying the ionic charge is essentially

equivalent to changing the dielectric constant or the temperature. In contrast to the standard RPM, for all ions, the charge will be located a distance, b , away from the hard-sphere centres of the particles. We shall denote our model as the Asymmetric Restricted Primitive Model (ARPM) and it is depicted in Figure 1. It should be noted that the ARPM is similar in spirit to a range of simple asymmetric models that were investigated by Spohr and Patey,¹⁻³ and by Lindenberg and Patey,^{4,5} although they included dispersion interactions, which we do not. We will generally consider fluids at room temperature (298 K), while Patey and co-workers primarily studied models at elevated temperatures. Furthermore, we will investigate the influence of b on fluid cohesion, and dielectric properties, which was not done in previous works.

Typical concentrations of RTILs are between 2 to 8 M. For example, bulk concentrations of *EMIBF₄*, *BPBF₄*, *EMITFSI* and *BPTFDSI* fall within the range 3.5 M - 6.5 M, at room temperature.²⁰ Hence, the diameter, d , should in our model be chosen to achieve this concentration, at a relatively high volume fraction. In this work, we set $d = 5$ Å. We will consider two different volume fractions: 0.49 and 0.23, corresponding to concentrations of about 6.2M and 2.9M, respectively. The more dense system has a volume fraction which is close to where the corresponding hard-sphere system would freeze. The less concentrated system is motivated by results obtained from NPT simulations at 1 bar, as we shall describe below.

The particles interact via a short-ranged repulsion which is the usual hard-sphere interaction in the MC simulations and a soft but steep potential in the MD simulations (details below). The Coulomb interaction energy, $u_{ij}(R)$ between charges i and j , separated a distance R , is given by,

$$u_{i,j}(R) = \frac{q_i q_j}{4\pi\epsilon_0\epsilon_\infty R} \quad (1)$$

where ϵ_0 is the dielectric permittivity of vacuum and ϵ_∞ is the high frequency contribution to the dielectric constant, stemming from electronic polarizability. We chose $\epsilon_\infty = 2$. In addition to the Coulomb interaction, there is a hard-sphere interaction, $u_{hs}(r)$ between hard-sphere centres i and

j , separated a distance r :

$$\beta u_{hs}(r) = \begin{cases} 0, & r > d \\ \infty, & r \leq d \end{cases} \quad (2)$$

In this work, we will consider two different simulation geometries. One uses cubic periodic boundary conditions to mimic a bulk solution. This system contains 800 ions, i.e. 400 neutral “salt pairs”, within a cubic simulation box, with a side length of either 47.5 Å (dense, 6.2 M, system) or 61 Å (less dense, 2.9 M, system). Cubic periodic boundary conditions were applied in all three dimensions.

The other system, with a spherical geometry, models a liquid droplet, and is used to determine the cohesive interactions in the fluid. In this case, 20000 ions were initially equilibrated inside a small droplet, with a hard confining boundary at a radius of 100 Å. This generates a fluid droplet with a relatively high volume fraction. After equilibration, the confining boundary was shifted out to a radius of 240 Å, causing an almost 14-fold increase of the system volume. If the fluid is very cohesive, essentially all particles will remain inside the original boundary, signifying a liquid with very low vapour pressure. In a less cohesive fluid, the droplet will evaporate, to give a uniform distribution of particles throughout the larger spherical volume. Droplets were only studied using MC. Note that since this is a limited system, there are no long-range “corrections”, i.e. the full Coulomb potential was utilized.

Ion pair definition

For increasing values of b , ions will show a greater tendency to form pairs with oppositely charged species. We then need a suitable definition of an ion pair. This will involve an inevitable ambiguity, but this is of small concern, given that we are primarily interested in how the ion pair fraction *changes* in the system. Given the propensity of the ions to form pairs, MC simulations of these systems become inefficient unless cluster moves²¹ are implemented. Note that, given the asymmetry, there are two relevant ion-ion separations:

- between hard-sphere centres (normally denoted r)

- between charges, denoted R

It is convenient to define the cluster (or ion pair) radius, R_{pair} , such that it is as large as possible, given the constraint that a cluster will contain at most two ions. In other words, if two particles have their charged sites at a distance less than R_{pair} , we shall define them as an ion pair. We then choose the value of R_{pair} such that, if two ions form a pair, then a third ion cannot simultaneously form a pair with either, due to steric repulsion. This leads to the following analytic expression:

$$R_{pair} = \sqrt{d^2 + b^2 - db\sqrt{3}} - b \quad (3)$$

An advantage with this definition, which is the one we have adopted, is that one only needs to scan for a single possible partner when performing a cluster move. Another advantage is that we ensure that each separate cluster is electroneutral and we can make comparisons with dipolar fluids, where the ion pairs are covalently bonded, permitting studies of dielectric response. Our definition means that the ion pair (cluster) radius, R_{pair} , will drop as b increases. This is illustrated in Figure 2.

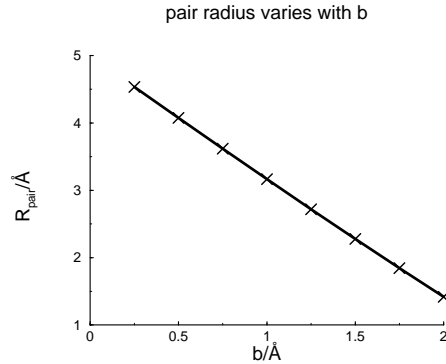


Figure 2: The variation of the ion pair radius with the asymmetry parameter b .

Note that our chosen definition rules out the existence of any ion pair in the RPM ($b = 0$). We stress that other definitions of ion pairs, or ion clusters, may offer some advantages, and may indeed be adopted in future work. Possibilities include definitions based on electrostatic binding energy, or to structural properties of radial distribution functions.

Metropolis Monte Carlo simulation details

The MC simulations utilized cluster moves, and single particle translation moves. In the latter case, the attempted translation was usually constrained to a spherical volume centred on the current position of the ion, but in one percent of the cases the attempted new location was chosen randomly within the simulation box. The long range part of the Coulomb interactions was handled via the so-called “SP3” splitting function, introduced by Fanourgakis.²² This approach closely resembles the so-called Wolf method,²³ but has the advantage that complementary error functions are avoided. We performed checks with simulations using the Wolf method, and observed no significant differences. The truncation radius was set to half the simulated box length of the system.

Molecular dynamics simulation details

All the MD simulations were performed using the software package LAMMPS²⁴. In order to avoid problems associated with impulsive forces due to hard sphere interactions, we adopted a smooth repulsive potential developed by Jover and co-workers²⁵. The so-called Mie potential is given by,

$$U(r) = \frac{\lambda_r}{\lambda_r - \lambda_a} \left(\frac{\lambda_r}{\lambda_a} \right)^{\frac{\lambda_a}{\lambda_r - \lambda_a}} \epsilon \left[\left(\frac{\sigma}{r} \right)^{\lambda_r} - \left(\frac{\sigma}{r} \right)^{\lambda_a} \right] \quad (4)$$

Setting $\lambda_r = 50$ and $\lambda_a = 49$, and truncating and shifting the potential at its minimum, results in the purely repulsive pseudo hard sphere potential:

$$U_{(50,49)}(r) = \begin{cases} 50 \left(\frac{50}{49} \right) \epsilon \left[\left(\frac{\sigma}{r} \right)^{50} - \left(\frac{\sigma}{r} \right)^{49} \right] + \epsilon, & r < \frac{50}{49} \sigma \\ 0, & r \geq \frac{50}{49} \sigma \end{cases} \quad (5)$$

We used $\epsilon = 50k_B T$ which gives a very steep potential, and σ is equal to the ARPM hard sphere diameter of 5 Å.

Electrostatic interactions were treated with the Ewald particle-particle particle-mesh method (PPPM),²⁶ with the real-space part of the Coulomb potential being truncated at 18 Å. The distance

between the center of the sphere and the point charge within the particle was constrained using the SHAKE algorithm.

All the simulations for the bulk systems were performed for 50 ns in the canonical ensemble, with a time step of 0.5 fs. The temperature was equal to 300 K, which was maintained via a Nose-Hoover thermostat, using a damping parameter of 100 fs.

Results and Discussion

We will present our results in three separate sections. The first section will focus on a dense bulk fluid. With ρ_+ and ρ_- denoting the cat- and anion densities, we then choose a volume fraction $\eta = (\rho_+ + \rho_-)\pi d^3/6$ such that it is close to the fluid-solid phase boundary ($\eta = 0.49$), for the corresponding hard-sphere system. Recall that for our ion diameter, this results in a salt concentration ($\rho_+ = \rho_-$) of about 6.2 M. In the subsequent section, we investigate the overall cohesive energy in the fluid, utilizing our droplet model. In the final section, we perform isobaric (NPT) simulations, at a pressure of 1 bar. The results from those simulations motivated further canonical ensemble simulations at approximately 2.9 M.

Dense bulk systems

Here we will investigate the ARPM with canonical ensemble simulations, using 800 ions, and a box length of $L_{box} = 47.5 \text{ \AA}$. This results in a volume fraction of about 0.49, which is close to the limit where a hard-sphere fluid will freeze. The corresponding concentration is approximately 6.2 M.

Melting point

First, we note that the RPM system (corresponding to b equal zero) freezes, under our room temperature conditions. This is clearly seen in Figure 3, where we show the projection of the particle coordinates on the $x - y$ plane, taken from a simulation snapshot of the RPM. The snapshot is from

an MD simulation, but a similar structure is obtained also by MC simulations, even when starting from randomly distributed coordinates. For some sufficiently large value of b the solid will melt into a fluid phase. This is obvious from the fact that, in the limiting case of b approaching the radius of the particles, we will arrive at a neutral dumbbell fluid ¹.

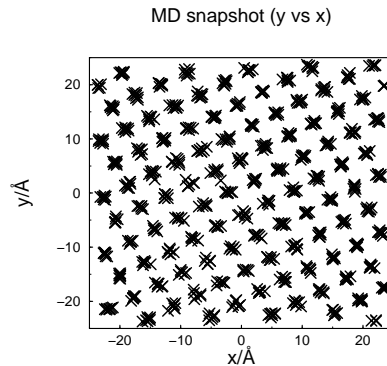


Figure 3: A snapshot of x, y coordinates, from an MD simulation snapshot

Structure

The transition from solid to fluid states can be traced by analyzing how the radial distribution function, $g(R)$, changes as b increases. Examples are shown in Figure 4.

¹It will be a fluid, since the volume fraction is chosen to be slightly below the freezing point of a hard-sphere fluid, and the corresponding dumbbell fluid will freeze at even higher volume fractions.

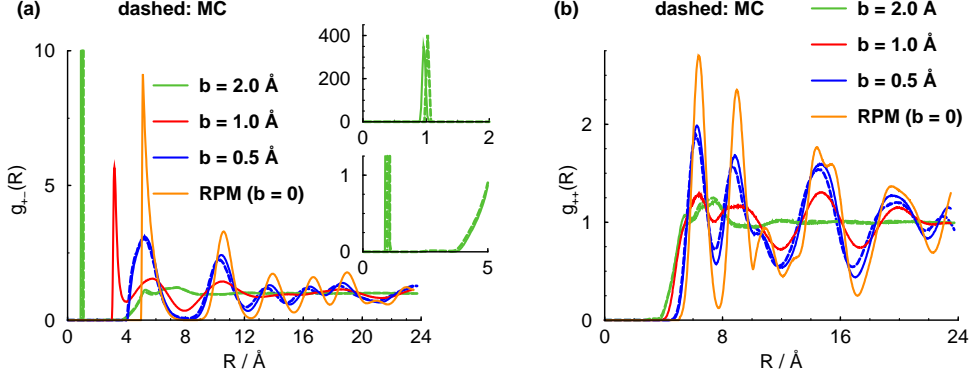


Figure 4: Radial distribution functions, for various degrees of charge asymmetry. Note that R measures the separation between charges. The insets of graph (a) zooms in on the primary peak, and the region between 1 and 5 Å, for the case $b = 2.0$ Å.

(a) Radial distribution function, $g_{+-}(R)$, between opposite charges

(b) Radial distribution function, $g_{++}(R)$, between positive charges

We note the expected long-ranged oscillations in the pair correlations, at low b -values, commensurate with an essentially frozen structure. Interestingly, the nearest-neighbour peak height for $g(R)_{+-}$ displays a non-monotonic dependence on b . The initial drop, at small b values, is perhaps best seen as a broadening of the peak, resulting from particle rotations. However, a further increase of b will generate strong orientational correlations, resulting in a dramatic increase of the peak height, combined with its shift to smaller separations. On the other hand, the long-ranged oscillations weaken monotonically as b is increased.

Dynamics

The degree of charge asymmetry also has a substantial impact on dynamics, as was also pointed out by Spohr and Patey.¹⁻³ However, in our dense canonical ensemble, room-temperature system the effect is rather dramatic, due to the system undergoing a phase transition (from a solid to liquid), as b increases from zero. In Figure 5, we see how the mean-square displacement, MSD , changes from insignificant values (as in a solid) to those typical of a fluid as b increases from 1.5 Å to 1.75 Å. The inset of Figure 5 shows focuses on the MSD for $b = 1.5$ Å. The observed initial increase can be attributed to local movements at sites within the solid. This increase is, as expected,

followed by an essentially constant MSD. Using the Einstein relation, the MSD values observed for $b = 1.75$ and 2.0 \AA , lead to predicted self diffusion coefficients of $3.5 * 10^{-6}$ and $6.5 * 10^{-6} \text{ cm}^2/\text{s}$, respectively. We conclude that for this volume fraction, and at room temperature, the system melts

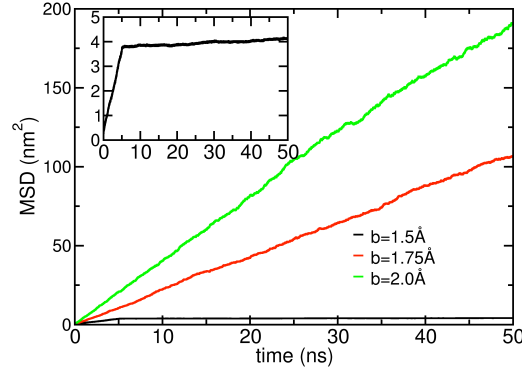


Figure 5: Plots of MD data on the mean square displacement, $MSD \equiv \langle |\mathbf{r}_\alpha(t) - \mathbf{r}_\alpha(0)|^2 \rangle^{1/2}$, where $r_\alpha(t)$ is the centre of mass coordinate for ion α , at time t . The brackets indicate a canonical average.

for asymmetries in the range $1.5 \text{ \AA} < b < 1.75 \text{ \AA}$.

Ion pairing

We expect that an increase in the asymmetry parameter b will also generate a higher fraction of ion pairs in the system (see above for the definition of an ion pair). This is illustrated in Figure 6 which displays the ion pair probability distributions, $P(X_{pair})$, for several values of b . Here, X_{pair} , is the molar fraction, of pairs. Note how there is a rather rapid transition from a dissociated to an almost completely associated system, occurring in the regime $0.5 \text{ \AA} < b < 1.5 \text{ \AA}$. The agreement between MC and MD results is not perfect, presumably reflecting the slight discrepancy between the models, but the qualitative outcomes are essentially the same.

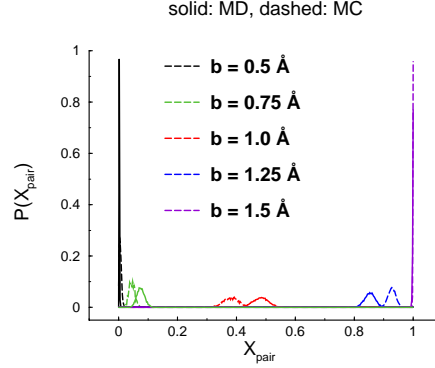


Figure 6: Ion pair probability profiles, for various degrees of charge asymmetry. X_{pair} is the mole fraction of ion pairs (see eq. (3)).

The maximum binding energy of a dimer pair, $e_B(max)$, is given by:

$$e_B(max) = \frac{q^2}{4\pi\epsilon_0\epsilon_\infty(d-2b)} \quad (6)$$

which rises rapidly, as b approaches $d/2$. Moreover, the shorter the bond length of the dimer the stronger will be the electrostatic attraction and this also enhances the stability of the dimers. All of this speaks for a rather sudden shift to a largely dimerized fluid as b increases.

Comparing with fluids of completely paired (dipolar) particles

As we have seen, almost all ions are paired for b values above about 1.5 Å. This suggests that these systems also could be modelled as a fluid of bonded (dipolar) pairs. The dipoles consist of a pair conformation that corresponds to perfect alignment of the charges (i.e. with the charges as close to each other as is permitted by the hard core constraint). We shall denote this bonded fluid as the “dipolar system”. We note then that in the dipolar system we have removed the option for partner exchange - a process that may occur even for high values of b in the ARPM. This notwithstanding, as illustrated in Figure 7, the average structure in the dipolar system agrees almost perfectly with the corresponding ARPM, with large enough charge asymmetry. This is consistent with similar findings by Ma *et al.* for model RTILs in slit geometries.²⁷

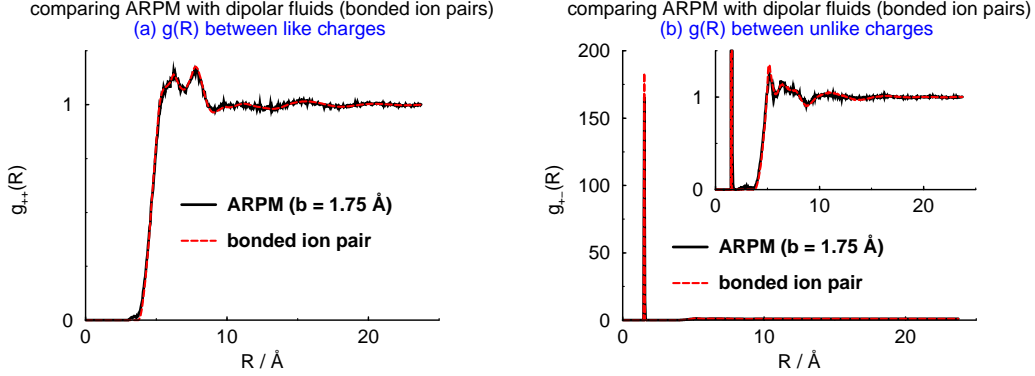


Figure 7: Comparing radial distribution functions for ARPM models, and their dipolar fluid counterpart. The dipolar fluid does not contain any free ions. Instead, it is composed of zwitterionic dipoles. These dipoles are formed by connecting ARPM ions, such as these become perfectly aligned, i.e. with the charges arranged as closely as possible, given the hard-sphere exclusion. Note that R measures the separation between charges.

(a) $g_{+-}(R)$

(b) $g_{++}(R)$

Dielectric properties of the dipolar system

The dipolar system is of course non-conducting, in contrast to typical RTILs, which generally have a small but finite conductivity. On the other hand, we recall that recent SFA measurements also suggest that there is an extremely low fraction of free ions present, at least in some RTILs. If this were the case, the ion pairs present would behave as a polar solvent with an inherent dielectric constant (which could be measured by applying an oscillating electric field of appropriate frequency). The RTIL would then be equivalent to a weak electrolyte with associated (long-ranged) electrostatic screening. The dielectric constant of the implicit ion paired solvent can be well approximated by that of the dipolar system (with the corresponding asymmetry parameter b), provided the free ion concentration is low. The absence of free ions in the dipolar system allows us to more easily calculate the dielectric response. In principle, one can estimate the dipolar contribution to the dielectric constant using dipole moment fluctuations of the simulation box.²⁸

Table 1: Simulated dielectric constants, $\langle \epsilon_r \rangle$, as obtained by applying a field along the z direction. The field results from placing an imaginary planar charged surface, with a uniform surface charge density $\sigma_s = 0.00025 \text{ e}/\text{\AA}^2$, extending infinitely in the (x, y) direction, at $z < -(L_{box} + d)/2$, and an oppositely charged surface at $z > (L_{box} + d)/2$ (their exact location is irrelevant). Here, e is the elementary charge. Two different system sizes were investigated.

$b/\text{\AA}$	$L_{box}/\text{\AA}$	$\langle \epsilon_r \rangle$
2.0	47.5	12
1.75	47.5	26
2.0	95.0	12
1.75	95.0	25

However, when we used this approach, the results obtained were very noisy, so we followed the suggestion by Kolafa *et al.* and applied an external field, E_z along the z direction. The total dielectric constant, ϵ_r of the system can then be obtained as:

$$\epsilon_r = \epsilon_r^\infty + \frac{\langle M_z \rangle}{\epsilon_0 E_z V} \quad (7)$$

where $V = L_{box}^3$ and $\langle M_z \rangle$ are the volume, and average dipole moment along the z direction, respectively, of the cubic simulation box. Table 1 gives the results obtained by applying fields of two different system sizes, using MC simulations. Even with this method, there is still some significant noise, but at least we can state that any system size dependence is small, and irrelevant to our main conclusion, namely that the dielectric response in the ARPM (with the given parameter choices) is typical to those of RTILs. Experimentally measured relative dielectric constants of real RTILs are often within the range 8-25. For instance, Huang *et al.*,²⁹ investigated a large number of RTILs, and reported values in the range 9-41, excluding the rather extreme (high) values obtained for RTILs with *OH*– functionalized cations.

Cohesion, droplet geometry

In order to investigate the role played by the asymmetry parameter b on the overall cohesion within the fluid, we performed MC simulations on a spherical droplet. The system was described in detail above. It consists of a dense spherical fluid droplet confined by a spherical boundary. The droplet was equilibrated within a smaller spherical boundary, which was then shifted outward.

The case for the RPM ($b = 0$) is illustrated in Figure 8 in the presence of the larger boundary. Clearly, there is sufficient cohesive energy in the system to maintain the integrity of the droplet. We investigated the effects of increasing the temperature in the RPM model system. Figure 8

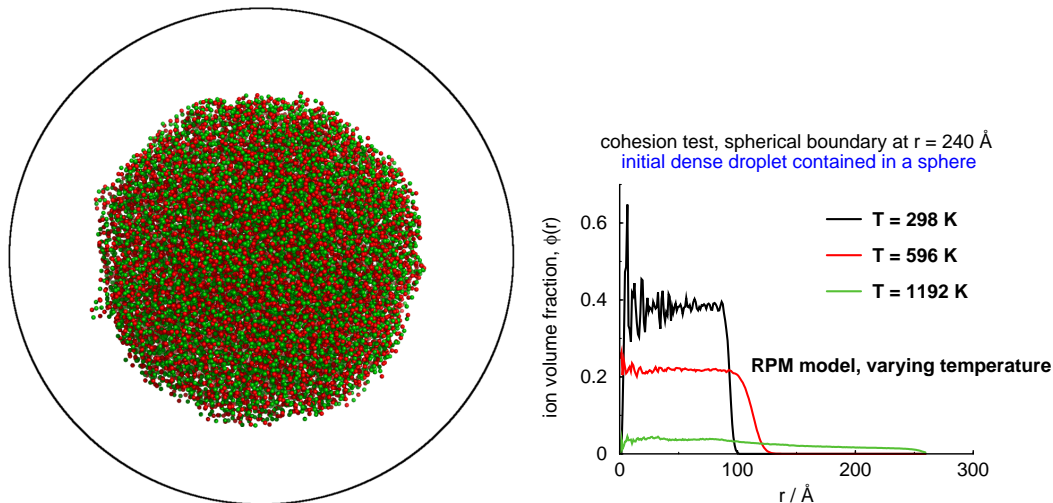


Figure 8: Left: a snapshot from a simulation of the RPM droplet. The confining outer boundary is indicated by a black circle. Right: radially dependent volume fractions, $\phi(r)$, for RPM systems, at different temperatures.

also shows the volume fraction profiles of the fluid as a function of the radial distance from the droplet center (at the center of mass). Doubling the temperature from 298 K to 596 K, leads to a decrease of the average density, but the droplet still remains condensed. Longer simulations of larger systems would in principle allow us to estimate the vapour pressure from the average density in the gas phase surrounding the condensed droplet. However, the vapour pressure is too low to be measurable for our system size, at these temperatures. At 1192 K, the droplet has evaporated completely. We now consider the corresponding ARPM systems, at room temperature but with varying b . The results are displayed in Figure 9. With $b = 1.0$ Å, the droplet remains condensed, with a very low (essentially unmeasurable) vapour pressure. An increase of the asymmetry, to $b = 1.5$ Å, leads to complete evaporation, with a gas phase filling the entire volume of the spherical cell. Thus, at room temperature, the cohesion of our ARPM is strong enough to support a condensed phase, with a very low vapour pressure, for modest values of b . However, somewhere in the regime

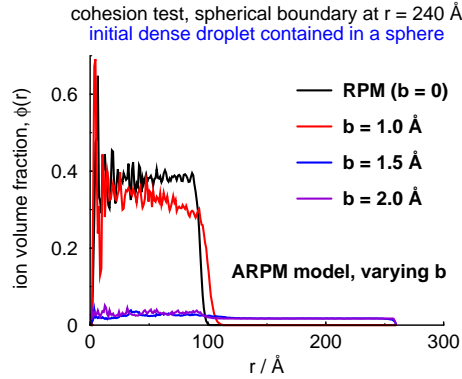


Figure 9: Radially dependent volume fractions, $\phi(r)$, for ARPM systems at room temperature, for different values of the asymmetry parameter b .

$1.0 \text{ \AA} < b < 1.5 \text{ \AA}$, the vapour pressure increases dramatically, and the fluid evaporates. As we shall see below, this is in line with our findings from isobaric bulk simulations.

Bulk systems at atmospheric pressure

As described earlier, we also carried out bulk *NPT* simulations at 1 bar and room temperature, utilizing MD. Comparable canonical ensemble MC simulations were also performed (for the case $b = 1.0 \text{ \AA}$) at the same average density as isobaric simulations.

Bulk densities from (*NPT*) simulations at 1 bar

We consider first how the average density responds to an increased charge asymmetry. In Figure 10, we see how the density only drops gradually for increased b provided $b \leq 1.0 \text{ \AA}$. In this range of asymmetry, the concentration remains liquid-like, with values that are typical for RTILs. However, asymmetries that are slightly larger than $b = 1.0 \text{ \AA}$, cause the liquid to evaporate. At much smaller values of b the system becomes crystalline. Combining these observations, have led us to more carefully explore the properties of the system with $b = 1.0 \text{ \AA}$. Here the ARPM would appear to have behaviors typical of RTILs.

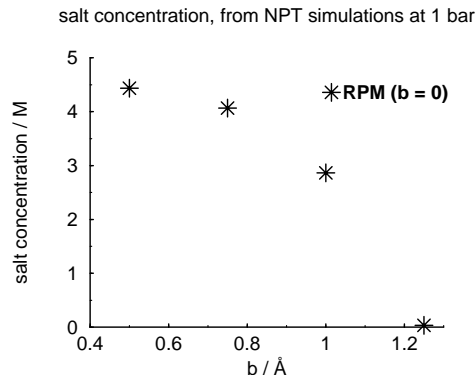


Figure 10: Average concentrations under ambient conditions (298 K, 1 bar), for various degrees of charge asymmetry.

The bulk fluid properties at atmospheric pressure, with $b = 1.0 \text{ \AA}$

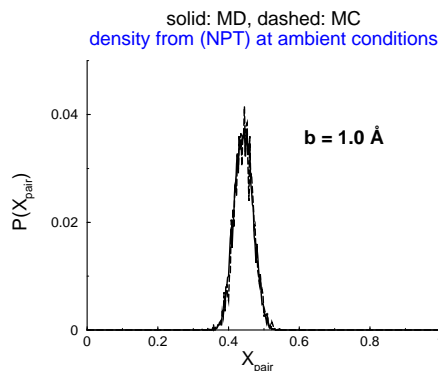


Figure 11: Ion pair probability distribution, for $b = 1.0 \text{ \AA}$, at a density for which the pressure is about 1 bar (at room temperature).

Here, we consider the special case of $b = 1.0 \text{ \AA}$, at a density that corresponds to a bulk pressure of 1 bar. We perform MC simulations in the canonical ensemble with 400 cations and 400 anions, which results in a simulation box with a side length of about 61 \AA . In Figure 11, we show the ion pair probability distribution, $P(X_{\text{pair}})$, for this system, as obtained by our canonical MC simulation, and compare it with the isobaric MD simulation (at 1 atm). We see that, on average, about half of the ions form pairs, under these conditions, which is consistent with typical estimates for bulk RTILs, as obtained by comparing measured conductivities with NMR data. [For instance, NMR](#)

measurements by Susan et al.²⁰ implied ion pair molar fractions in the range 0.2-0.9 for, *EMIBF₄*, *BPBF₄*, *EMITFSI* and *BPTFDSI*. Using MD simulations, we have also calculated the conductivity, as well as the self-diffusion coefficient (see specific values reported below). The conductivity is measured via the Green-Kubo relation, by integrating the electric current autocorrelation function,

$$\sigma = \frac{1}{3k_BTV} \int_0^\infty \langle \mathbf{J}(0)\mathbf{J}(t) \rangle dt \quad (8)$$

where V is the volume of the simulation box, while $\mathbf{J}(t)$ is the electric current at time t , which is calculated via $\mathbf{J}(t) = \sum_{i=1}^N q_i \mathbf{v}_i$. Here, q_i is the charge of the particle i , and \mathbf{v}_i is the velocity.

In summary, we find that this particular ARPM system:

- is a dense fluid at room temperature and atmospheric pressure, with a concentration (2.9M) that falls inside the range of typical values for RTILs
- is composed of ions of which about 50 percent form ion pairs - in agreement with experimental bulk RTIL estimates
- has a conductivity of about 12 S/m, which is a realistic, albeit high, value for RTILs
- has a self-diffusion constant of about $8.7\text{e-}5 \text{ cm}^2/\text{s}$, which is 1-2 orders of magnitude higher than for typical RTILs

An unrealistically rapid diffusion is not unexpected, given the idealized spherical geometry of the ions. Nevertheless, even though the ARPM is coarse-grained and somewhat simplistic it nevertheless does reproduce some properties of typical RTILs remarkably well, indicating that it captures some of the important physics in these systems.

Conclusions

We have introduced and investigated some properties of the ARPM, which results from a minor modification of the RPM. In the ARPM, a single new parameter, b , is used, which measures the

displacement of the ionic charge from the center of the hard sphere. Such a displacement uniformly applied to all particles creates a model, which, while simple, introduces a mechanism that extends the applicability of the RPM to a wider range of realistic systems, including RTILs. The presence of a non-vanishing displacement b means that the ions of the system now have an internal structure and orientations can become correlated. Larger b also increases the possibility of dimers of oppositely charged ions.

In this work, the fundamental bulk properties of the ARPM, such as structure and phase stability, as well as dynamic properties, such as conductivity and diffusion have been investigated. Despite the simplicity of the model, it is able to generate remarkably realistic properties, compared with real RTILs, suggesting that it does capture most of the important physics that underlies some of the fascinating properties displayed by RTILs. The simplicity of the ARPM also offer important modelling advantages. The computational cost is minimal, as compared with more elaborate, or even all-atomistic models. Furthermore, the simple structure of the ARPM should facilitate analyses by more approximate theoretical approaches, such as integral equations, or statistical density functional theory.

Future studies will include the behaviour of the ARPM in heterogeneous systems, such as in the vicinity of electrodes. [As mentioned earlier, we also anticipate that the ARPM will form an interesting extension to the RPM description of aqueous electrolyte solutions.](#)

Acknowledgments

We acknowledge the Marie-Curie NanoS3 project from EU for financial support, and LUNARC for generous computational allocation. J.F. also acknowledges financial support from the Swedish Research Council.

References

1. Spohr, H.; Patey, G. Structural and dynamical properties of ionic liquids: The influence of ion size disparity. *The Journal of chemical physics* **2008**, *129*, 064517.
2. Spohr, H. V.; Patey, G. Structural and dynamical properties of ionic liquids: competing influences of molecular properties. *The Journal of chemical physics* **2010**, *132*, 154504.
3. Spohr, H. V.; Patey, G. The influence of water on the structural and transport properties of model ionic liquids. *The Journal of chemical physics* **2010**, *132*, 234510.
4. Lindenberg, E. K.; Patey, G. N. How distributed charge reduces the melting points of model ionic salts. *The Journal of Chemical Physics* **2014**, *140*.
5. Lindenberg, E. K.; Patey, G. N. Melting point trends and solid phase behaviors of model salts with ion size asymmetry and distributed cation charge. *The Journal of Chemical Physics* **2015**, *143*.
6. Malvaldi, M.; Chiappe, C. From molten salts to ionic liquids: effect of ion asymmetry and charge distribution. *Journal of Physics: Condensed Matter* **2008**, *20*, 035108.
7. Silvestre-Alcantara, W.; Bhuiyan, L.; Lamperski, S.; Kaja, M.; Henderson, D. Double layer for hard spheres with an off-center charge. *arXiv preprint arXiv:1603.02172* **2016**,
8. Silvestre-Alcantara, W.; Henderson, D.; Wu, J.; Kaja, M.; Lamperski, S.; Bhuiyan, L. B. Structure of an electric double layer containing a 2:2 valency dimer electrolyte. *Journal of Colloid and Interface Science* **2015**, *449*, 175 – 179.
9. Fedorov, M. V.; Kornyshev, A. A. Ionic Liquid Near a Charged Wall. Structure and Capacitance of Electrical Double Layer. *The Journal of Physical Chemistry B* **2008**, *112*, 11868–11872, PMID: 18729396.
10. Fedorov, M.; Georgi, N.; Kornyshev, A. Double layer in ionic liquids: The nature of the camel shape of capacitance. *Electrochemistry Communications* **2010**, *12*, 296 – 299.

11. Gebbie, M. A.; Valtiner, M.; Banquy, X.; Fox, E. T.; Henderson, W. A.; Israelachvili, J. N. Ionic liquids behave as dilute electrolyte solutions. *Proceedings of the National Academy of Sciences* **2013**, *110*, 9674–9679.
12. Gebbie, M. A.; Dobbs, H. A.; Valtiner, M.; Israelachvili, J. N. Long-range electrostatic screening in ionic liquids. *Proceedings of the National Academy of Sciences* **2015**, *112*, 7432–7437.
13. Fry, A. J. Strong ion-pairing effects in a room temperature ionic liquid. *Journal of Electroanalytical Chemistry* **2003**, *546*, 35 – 39.
14. Fraser, K. J.; Izgorodina, E. I.; Forsyth, M.; Scott, J. L.; MacFarlane, D. R. Liquids intermediate between "molecular" and "ionic" liquids: Liquid Ion Pairs? *Chem. Commun.* **2007**, 3817–3819.
15. Kirchner, B.; Malberg, F.; Firaha, D. S.; Holloczki, O. Ion pairing in ionic liquids. *Journal of Physics: Condensed Matter* **2015**, *27*, 463002.
16. Smith, A. M.; Lee, A. A.; Perkin, S. The Electrostatic Screening Length in Concentrated Electrolytes Increases with Concentration. *The Journal of Physical Chemistry Letters* **2016**, *7*, 2157–2163, PMID: 27216986.
17. Zhang, Y.; Maginn, E. J. Direct Correlation between Ionic Liquid Transport Properties and Ion Pair Lifetimes: A Molecular Dynamics Study. *The Journal of Physical Chemistry Letters* **2015**, *6*, 700–705, PMID: 26262489.
18. Sha, M.; Dong, H.; Luo, F.; Tang, Z.; Zhu, G.; Wu, G. Dilute or Concentrated Electrolyte Solutions? Insight from Ionic Liquid/Water Electrolytes. *The Journal of Physical Chemistry Letters* **2015**, *6*, 3713–3720, PMID: 26713896.
19. Holloczki, O.; Malberg, F.; Welton, T.; Kirchner, B. On the origin of ionicity in ionic liquids. Ion pairing versus charge transfer. *Phys. Chem. Chem. Phys.* **2014**, *16*, 16880–16890.

20. Susan, M. A. B. H.; Noda, A.; Watanabe, M. In *Electrochemical Aspects of Ionic Liquids, Second Edition*; Ohno, H., Ed.; Wiley: New York, 2011; pp 65–85.
21. Wu, D.; Chandler, D.; Smit, B. Electrostatic analogy for surfactant assemblies. *The Journal of Physical Chemistry* **1992**, *96*, 4077–4083.
22. Fanourgakis, G. S. An Extension of Wolfs Method for the Treatment of Electrostatic Interactions: Application to Liquid Water and Aqueous Solutions. *The Journal of Physical Chemistry B* **2015**, *119*, 1974–1985, PMID: 25611255.
23. Wolf, D.; Keblinski, P.; Phillpot, S. R.; Eggebrecht, J. Exact method for the simulation of Coulombic systems by spherically truncated, pairwise $\frac{1}{r}$ summation. *The Journal of Chemical Physics* **1999**, *110*, 8254–8282.
24. Plimpton, S. Fast Parallel Algorithms for Short-Range Molecular Dynamics. *J. Comput. Phys.* **1995**, *117*, 1–19.
25. Jover, J.; Haslam, A. J.; Galindo, A.; Jackson, G.; Müller, E. A. Pseudo hard-sphere potential for use in continuous molecular-dynamics simulation of spherical and chain molecules. *J. Chem. Phys.* **2012**, *137*, 144505.
26. Plimpton, S.; Pollock, R.; Stevens, M. In *Proceedings of the Eighth SIAM Conference on Parallel Processing for Scientific Computing*; 1997.
27. Ma, K.; Forsman, J.; Woodward, C. E. Influence of ion pairing in ionic liquids on electrical double layer structures and surface force using classical density functional approach. *The Journal of Chemical Physics* **2015**, *142*, 174704.
28. Neumann, M. Dipole moment fluctuation formulas in computer simulations of polar systems. *Molecular Physics* **1983**, *50*, 841–858.
29. Huang, M.-M.; Jiang, Y.; Sasisanker, P.; Driver, G. W.; Weingärtner, H. Static Relative

Dielectric Permittivities of Ionic Liquids at 25 °C. *Journal of Chemical & Engineering Data* **2011**, 56, 1494–1499.